University of South Carolina
Scholar Commons

Theses and Dissertations

Summer 2021

Simulation of Pituitary Organogenesis in Two Dimensions

Chace E. Covington

Follow this and additional works at: https://scholarcommons.sc.edu/etd

 Part of the Mathematics Commons

Recommended Citation

Covington, C. E.(2021). *Simulation of Pituitary Organogenesis in Two Dimensions.* (Master's thesis). Retrieved from https://scholarcommons.sc.edu/etd/6450

This Open Access Thesis is brought to you by Scholar Commons. It has been accepted for inclusion in Theses and Dissertations by an authorized administrator of Scholar Commons. For more information, please contact dillarda@mailbox.sc.edu.

Simulation of Pituitary Organogenesis in Two Dimensions

by

Chace E. Covington

Bachelor of Science
Francis Marion University 2019

Submitted in Partial Fulfillment of the Requirements

for the Degree of Master of Science in

Mathematics

College of Arts and Sciences

University of South Carolina

2021

Accepted by:

Paula Vasquez, Major Professor

Shannon Davis, Committee Member

Tracey L. Weldon, Interim Vice Provost and Dean of the Graduate School

© Copyright by Chace E. Covington, 2021
All Rights Reserved.

Abstract

The pituitary gland is a vital part of the endocrine system found in all vertebrates and is responsible for the production of hormones that influence many physiological processes in the organism's body. Although much has been learned of pituitary organogenesis, studying the dynamics of the cells in the developing pituitary gland is difficult. Pituitary organogenesis has been studied through "snapshots" of a developing pituitary gland by removing and viewing the pituitary glands of different specimens. Thus, how the individual cells in the developing pituitary gland behave and interact with one another is not fully understood. To aid in understanding pituitary organogenesis, we created a computational model to simulate the proliferation of stem cells in the pituitary gland of a mouse and the effects of forces acting on those cells as the pituitary gland develops. This model focuses on the proliferation and dynamics of stem cells in the pituitary gland once Rathke's pouch has formed a ring structure separate from the oral ectoderm. This model represents cells as polygons with a finite number of vertices, where forces acting on the cell will be represented as a force acting on the vertices of the cell. The forces simulated in this model and the simulation of cellular proliferation will be discussed in detail.

Contents

List of Figures

Introduction

The pituitary gland is an organ found in all vertebrates and is a vital part of the endocrine system. Found beneath the hypothalamus, the pituitary gland produces hormones that regulate many physiological processes in the organism, including growth, metabolism, and the reproductive system. The anterior lobe of the pituitary gland develops in a fetus from the oral ectoderm (Shields et al. 2015). Stem cells in the oral ectoderm fold into an elliptical structure—referred to as Rathke's pouch—with a central lumen. The stem cells will proliferate and differentiate around the luminal area before migrating anteriorly to form the anterior lobe and differentiate into hormone producing cell types (Scully and Rosenfeld 2002).

As the pituitary gland is a vital part of the endocrine system, there has been much research done on its development. However, to study the development of the pituitary gland through experimental data, a sample from a developing fetus must be taken, creating difficulties. For example, Youngblood et al. studied pituitary organogenesis in mice, and samples of developing brain tissue were extracted from mice fetuses (Youngblood, Coleman, and Davis 2018). However, this halts the development of the pituitary gland, and pituitary organogenesis can only be studied through "snapshots" taken from different fetuses at different stages in development. This thesis proposes a mathematical model that can simulate the proliferation of stem cells in a simplified Rathke's pouch to provide information on the processes that take place between the "snapshots" used thus far to observe the development of the anterior lobe of the pituitary gland. This model will add signalling gradients of signalling proteins influencing proliferation described by Scully (Scully and Rosenfeld 2002) to the cellular dynam-

ics models developed by Boromand et al. (Boromand et al. 2018) and Fletcher et al. (Fletcher et al. 2013). Thus, this model will test whether the signalling gradients of signalling proteins influencing proliferation determines the final shape of the anterior lobe.

This model includes the effects of two different proteins: fibroblast growth factor (FGF) and sonic hedgehog (SHH). Two forms of FGF—FGF8 and FGF10—are active around Rathke's pouch (Scully and Rosenfeld 2002), but this model makes no distinction between the two different forms. Although FGF and SHH can influence multiple aspects of pituitary organogenesis (Scully and Rosenfeld 2002), the only effect of these proteins that is within the scope of this model is their effect on cellular proliferation. Stem cells under the influence of FGF and/or SHH have increased rates of cellular division. This model uses three sources of FGF and SHH: one source of FGF and one source of SHH from the infundibular region of the ventral diencephalon and one source of SHH from the oral ectoderm. Because Rathke's pouch separates from the oral ectoderm, the source of SHH from the oral ectoderm disappears, with its effects weakening over time in the model. These sources of FGF and SHH create a signalling gradient, and the affect these proteins have on a cell is dependent on the location of the cell relative to the source of the protein (Scully and Rosenfeld 2002).

In this model, cells will be in one of three phases in the cell-division cycle: interphase, mitosis, or G_0. In interphase, a cell will grow in size and develop the materials necessary for cellular division. Once a cell completes interphase, the cell enters mitosis and will begin the cellular division process. Once the cell completes mitosis, the cell will have divided into two separate cells. If a cell has completed mitosis and the two resulting cells are still able to divide, then those cells reenter interphase and begin the cell-division cycle again. A cell that is not preparing for division has exited the cell cycles. Cells that have exited the cell cycle are referred to as G_0.

Chapter 1

Introduction to Model

1.1 Representation of Cells and Initial Condition

The representation of a cell in this model is similar to the structure of deformable polygons in Boromand's "Jamming of Deformable Polygons" (Boromand et al. 2018). Figure 1.1 depicts the graphical representation of a single cell in the model. Each cell consists of a collection of vertices, and, excluding cellular division, these vertices will remain associated with this cell. Vertices cannot be shared between multiple cells. The number of vertices for each cell is not uniform, so different cells may each have a different amount of vertices. Outside of cellular division, no new vertices will be created for a cell, and no vertices will be deleted in the simulation.

The simulation begins once Rathke's pouch has separated from the oral ectoderm. Figure 1.2 depicts the initial condition of the stem cells in the simulation as a cross-section of the developing pituitary gland such that the positive direction in the y-axis is the posterior direction, and the positive direction in the x-axis is the dorsal direction. As time progresses the stem cells will proliferate, and more cells will be produced.

1.2 Representation of Cellular Division and Signalling Gradients

When a cell completes mitosis, the one cell will divide into two cells. When a cell divides, each resulting cell will retain some of the vertices of the original cell. Figure 1.3 depicts the results of a cell dividing. The cell will divide along the shortest chord

that crosses through the centroid of the cell. New vertices will be formed in what was the interior of the original cell, following lines parallel to the shortest the chord that crosses through the centroid. The two cells resulting from the division will be roughly half of the size of the original cell. Neither of the resulting cells will necessarily have the same number of vertices as the original cell, nor will they necessarily have the same number of vertices as each other.

The signalling gradients for FGF and SHH will emanate from a line segment for FGF and point sources for SHH. A cell will be influenced by FGF and/or SHH if the centroid of the cell is within a specified radius of the source. Figure 1.4 depicts the placement of the signalling gradients relative to the cells in the initial condition. All of the cells in Figure 1.4 whose centroids fall within at least one of the areas of effect for FGF and SHH will be affected by the respective protein(s). Cellular division in the model will be discussed in the Chapter 3.

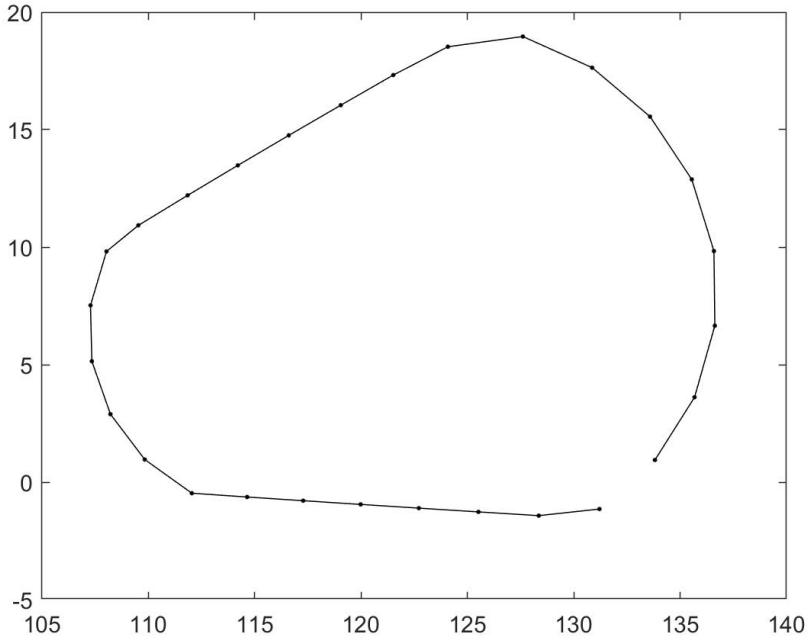

Figure 1.1 Depiction of cell as represented in the model

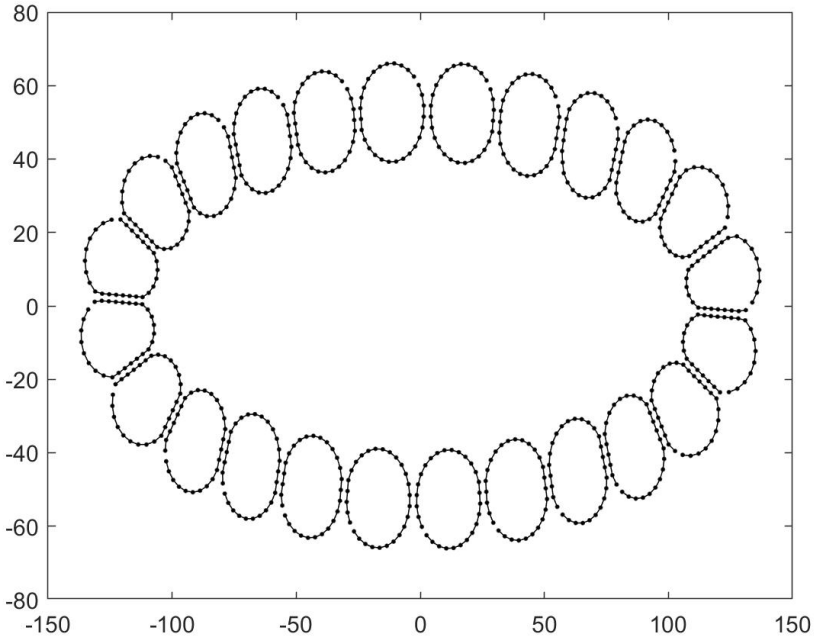

Figure 1.2 Initial layout of cells at the start of the simulation. Note that each cell consists of a collection of vertices.

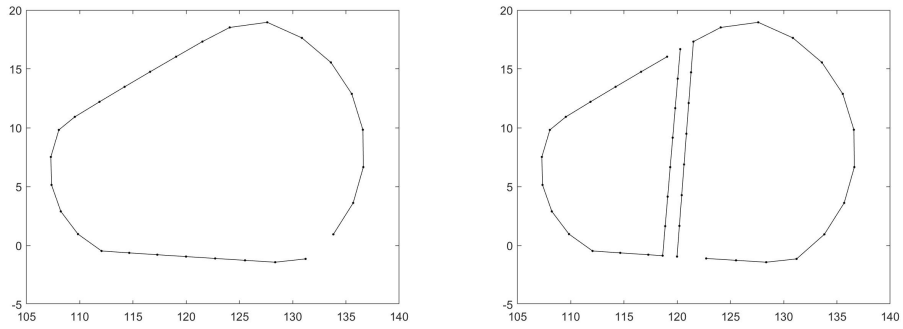

Figure 1.3 (Left) Cell before undergoing division. (Right) Resulting daughter cells after a the cell undergoes cellular division.

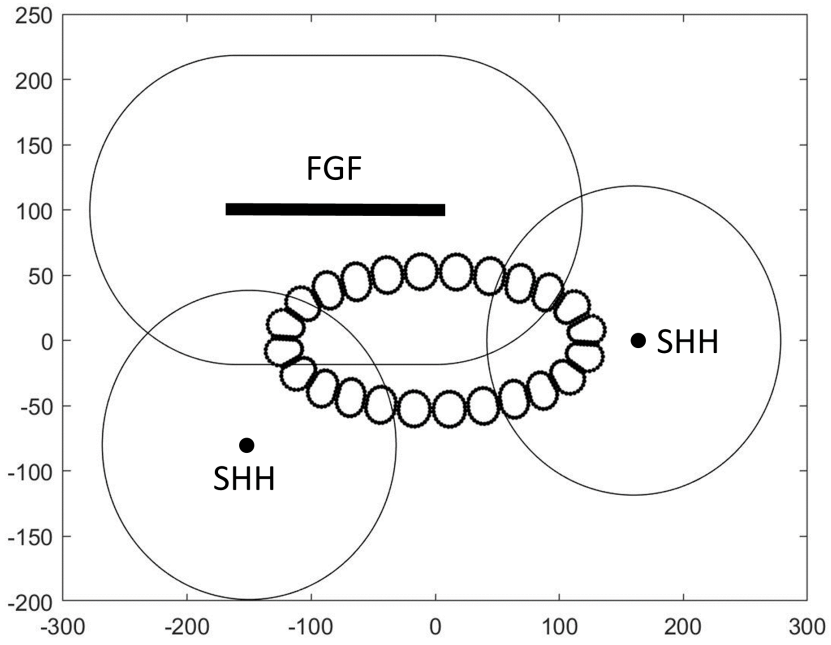

Figure 1.4 Graph of signalling gradients for FGF and SHH with initial condition. The SHH point sources are located at (-150,-80) and (160,0), and the vertices for the FGF line segment source are located at (-160,100) and (0,100). The area of effect for SHH is represented by the two circles, and the area of effect for the FGF is the curve resembling an ellipse.

Chapter 2

Dynamics of the Cells

2.1 Overview of Dynamics in Model

The motion of the cells are simulated using the processes discussed in papers by Boromund (Boromand et al. 2018) and by Fletcher (Fletcher et al. 2013). The motion of the ith vertex is determined by Eq. (1) in Fletcher et al. (Fletcher et al. 2013), which is the differential equation

$$\eta_i \frac{d\mathbf{r}_i}{dt} = \mathbf{F}_i, \tag{2.1}$$

where η_i is the drag coefficient, $\mathbf{r}_i$ is the position of the vertex, and $\mathbf{F}_i$ is the net force acting on the vertex. We can solve Eq. (2.1) computationally using a simple forward Euler discretization (Fletcher et al. 2013).

The forces exerted on the vertices of the cells can be categorized as either vertex-unique forces and cell-unique forces. Vertex-unique forces are forces that depend on the position of the specific vertex relative to the other vertices of both its cell and the vertices of the other cells. Thus, the vertex-unique forces will not be uniform for all vertices in a cell. Cell-unique forces are forces that depend on the position of the cell relative to the other cells. Thus, the cell-unique forces will be uniform for all vertices in a cell, although the cell-unique forces will be different for each cell.

The vertex-unique forces are the area force, the contractile force, and the excluded volume force. The calculation of these vertex-unique forces are derived from Eq. (1) of the supplemental material from "Jamming of Deformable Polygons" (Boromand et al. 2018). The area force is a repellent force that prevents the vertices from a single

cell from converging into one point, effectively meaning the cell has shrunk into a single point. The contractile force is an attractive force that prevents the vertices from a single cell from spreading out too far, limiting the growth of the area of the cell. The excluded volume force is a repellent force that prevents a cell from folding over itself or from two cells overlapping.

The cell-unique forces are the neighbor force and the central force. These two forces were developed for this simulation. The neighbor force is a force that simulates the weak attachment between neighboring cells in the pituitary gland. The neighbor force treats the interaction between two neighboring cells as a spring. Thus, the neighbor force is an attractive force between two cells if the cells are too far away from one another and is a repellent force if the cells are too close together. The central force is a force that simulates the force of the material outside of the pituitary gland and the fluid inside the lumen pushing on the cells in the pituitary gland. The central force treats each cell as a mass on a spring where the equilibrium length is relative to the position of the cell and the center of the lumen. Thus, the central force attracts the cell towards the center of the lumen if the cell is too far away from the center, and it repels the cell from the center of the lumen if the cell is too close to the center.

Consider the ith vertex at position $\mathbf{r}_i$. Then we can define the net force acting on that vertex using the vertex-unique and cell-unique forces through the following equation:

$$\mathbf{F}_i = \mathbf{A}_i + \mathbf{S}_i + \mathbf{V}_i + \mathbf{N}_i + \mathbf{C}_i, \tag{2.2}$$

where $\mathbf{A}_i$ is the area force, $\mathbf{S}_i$ is the contractile force, $\mathbf{V}_i$ is the excluded volume force, $\mathbf{N}_i$ is the neighbor force, and $\mathbf{C}_i$ is the central force.

By solving Eq. (2.1) for $d\mathbf{r}_i$, using that to update a vertex's position from time j to time $j+1$, and substituting the result from Eq. (2.2), one forms the equation

$$\mathbf{r}_i^{(j+1)} = \mathbf{r}_i^{(j)} + \frac{dt}{\eta_i}\left(\mathbf{A}_i^{(j)} + \mathbf{S}_i^{(j)} + \mathbf{V}_i^{(j)} + \mathbf{N}_i^{(j)} + \mathbf{C}_i^{(j)}\right), \tag{2.3}$$

where the superscript (j) in each term denotes that term at time j.

2.2 Area Force

A cell's size is determined by many outside factors, especially nutrient levels (Björklund and Marguerat 2017). This model does not account for any specific factors that affect a cell's size. Instead, the area force and contractile force, which will be discussed in the next section, are used to regulate the size of each cell. The area force is primarily used to prevent a cell from becoming too small. An equilibrium area for the cell is defined, and the dynamics of the cell as it expands or contracts to achieve that equilibrium area is similar to a spring system. The area force will expand the cell if the cell has an area below the equilibrium area, and the it will shrink the cell if the cell has an area above the equilibrium area. For most situations in the simulation, the area force will expand the cell.

The area force $\mathbf{A}$ is defined by

$$\mathbf{A}_i = \frac{k_a}{dt}\left(\mathbf{c} - \mathbf{r}_i\right)\left(1 - \frac{a_0}{a}\right), \tag{2.4}$$

where $\mathbf{c}$ is the center of mass of the cell containing the ith vertex, k_a is a spring constant that helps determine how quickly the cell will expand, a is the area of the cell, and a_0 is the equilibrium area for the cell.

Figure 2.1 depicts how changes in the equilibrium area affects the area force's effect on a cell. Each cell began with the same initial condition, and the area force was used to update the position of each vertex for each time step. It can be seen that increasing the value of a_0 strengthens the area force as a repulsive force, allowing for larger cells.

2.3 Contractile Force

Along with the area force, the contractile force is used to regulate the size of the cells. Unlike the area force, the contractile force is primarily used to prevent a cell from becoming too large. An equilibrium length between two consecutive vertices in a cell is defined, and the dynamical system between consecutive vertices is treated as two masses connected by a spring. If the distance between two consecutive vertices in a cell is smaller than the defined equilibrium length, the vertices will repel one another, and if the distance between the two consecutive vertices is larger than the equilibrium distance, the vertices will attract one another. For most situations in the simulation, the contractile force will attract consecutive vertices to one another, shrinking the overall cell.

The contractile force $\mathbf{S}$ is defined by

$$\mathbf{S}_i = k_\ell \left(\sum_{j=1}^{N} \sqrt{\mathbf{r}_j \cdot \mathbf{r}_{\bar{j}}} - \ell_0 \right) \left(\frac{\mathbf{r}_i - \mathbf{r}_{\text{next}}}{||\mathbf{r}_i - \mathbf{r}_{\text{next}}||} + \frac{\mathbf{r}_i - \mathbf{r}_{\text{prev}}}{||\mathbf{r}_i - \mathbf{r}_{\text{prev}}||} \right), \tag{2.5}$$

where N is the number of vertices in the cell, $r_{\bar{j}}$ denotes the $j+1$th vertex in the cell (or vertex 1 if $j = N$), $||\cdot||$ denotes the Euclidean norm, k_ℓ is a spring constant, ℓ_0 is the equilibrium length between two consecutive vertices, $\mathbf{r}_{\text{next}}$ denotes the $i+1$th vertex (or vertex 1 if $i = N$), and $\mathbf{r}_{\text{prev}}$ denotes the $i-1$th vertex (or the Nth vertex if $i = 1$).

Figure 2.2 depicts the the impact the value of ℓ_0 has on the strength of the contractile force. Each cell started with the same initial condition, and the contractile force was used to update the position of each vertex for each time step. It can be seen that increasing the value of ℓ_0 strengthens the contractile force, shrinking the cells.

2.4 Excluded Volume Force

When two cells are touching each other, the cell membranes of both cells prevent the cells from overlapping one another. The excluded volume force is primarily used to prevent such overlapping as well as to prevent vertices from colliding with one another. The calculation of the excluded volume force between two vertices is similar to a gaussian function. The closer two vertices are to one another, the stronger the excluded volume force between those two vertices will be. The excluded volume force will always be a repulsive force.

The excluded volume force $\mathbf{V}_i$ is defined by

$$\mathbf{V}_i = \sum_{k=1}^{N} \left((\mathbf{r}_k - \mathbf{r}_i) \exp\left(-\frac{||\mathbf{r}_i - \mathbf{r}_k||^2}{d_{min}^2} \right) \right), \tag{2.6}$$

where d_{min} is the minimum distance between line segments of neighboring cells (Boromand et al. 2018) and $|| \cdot ||$ is the Euclidean norm.

Figure 2.3 depicts how changes in the d_{min} value affects the excluded volume force's effect on the cells. Each simulation consisted of three cells, and each simulation had the same initial condition. The excluded volume force was used to update the position of the vertices for each time step. It can be seen from the figure that increasing the value of d_{min} increases the strength of the excluded volume force as a repulsive force, resulting in larger cells and larger distances in-between cells.

2.5 Neighbor Force

As the pituitary gland develops, stem cells are attached to nearby stem cells in an epithelium connected by tight junctions (Wilfinger et al. 1984). The neighbor force is a force that simulates this connection. The model simulates the attachment of cells as a spring connecting two neighboring cells. The neighbor force between two cells will be nonzero only if the cells are neighbors. Thus, cells who are not considered neighbors will not contribute to the calculation of each other's neighbor force. Let

there be N cells, and consider the ith and jth cells. Let $\mathbf{c}_n$ denote the position of the centroid of the nth cell and $||\cdot||$ denote the Euclidean norm. Then the ith and jth cells are neighbors if the following inequality is true:

$$||\mathbf{c}_i - \mathbf{c}_j|| \leq 1.5 \min\left(\min_{n\in[1,N]} ||\mathbf{c}_i - \mathbf{c}_n||, \min_{n\in[1,N]} ||\mathbf{c}_j - \mathbf{c}_n||\right). \tag{2.7}$$

The neighbor force $\mathbf{N}$ for every vertex in the ith cell is defined by

$$\mathbf{N}_i = -k_n \sum_{j=1}^{N} \left((\mathbf{c}_i - \mathbf{c}_j)\left(1 - 2a_0 ||\mathbf{c}_i - \mathbf{c}_j||^{-1}\right)\right), \tag{2.8}$$

where N is the number of neighboring cells to the ith cell, k_n is the spring constant, and $\mathbf{c}_i$ is the center of mass of the ith cell.

Figure 2.4 depicts the effects changing the value of the spring constant has on the neighbor force. Every simulation began with the same initial conditions, and the neighbor force was used to update the position of the vertices at each time step. It can be seen that increasing the spring constant strengthens the neighbor force.

2.6 Central Force

As discussed in the Introduction, Rathke's pouch is a collection of stem cells that surround a lumen. The fluid inside the lumen will push outwards on the stem cells in Rathke's pouch. As Rathke's pouch is surrounded by other tissues, the stem cells will also be pushed from the outside of Rathke's pouch by this surrounding tissue. The central force addresses both the pressure from the fluid in the lumen and the pressure from the tissue surrounding Rathke's pouch by treating the system as a mass on a spring. An equilibrium distance from the center of the lumen is defined, and the magnitude and direction of the central force acting on a cell will depend on the distance between the cell's centroid and the center of the lumen. If the distance between a cell's centroid and the center of the lumen is smaller than the equilibrium distance, then the central force will push the cell away from the center of the lumen,

simulating the fluid in the lumen pushing outward on the cells in Rathke's pouch. If the distance between a cell's centroid and the center of the lumen is larger than the equilibrium distance, then the central force will push the cell towards the center of the lumen, simulating the outside tissue pushing on the stem cells from outside Rathke's pouch.

The central force $\mathbf{C}$ for every vertex in the ith cell is defined by

$$\mathbf{C}_i = -k_c \mathbf{c}_i \left(1 - \ell_c\right), \tag{2.9}$$

where k_c is the spring constant, $\mathbf{c}_i$ is the center of mass for the ith cell, and ℓ_c is the equilibrium distance from the center of the pituitary gland.

Figure 2.5 depicts the effect changing the equilibrium distance has on the central force. Each simulation started with the same initial conditions, and the position of the vertices were updated each time step using the central force. Note that increasing the equilibrium distance forces the cells farther apart.

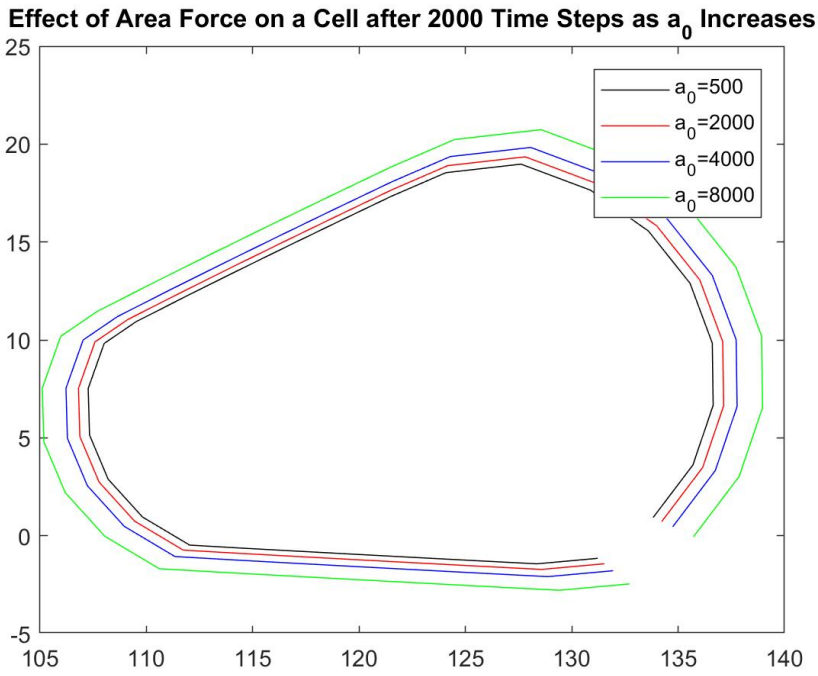

Figure 2.1 Graph showing how the value of a_0 affects the area force. Each cell started with the same initial condition, and the area force was used to update the positions of the vertices for 2000 time steps. Note that as the value of a_0 increases, the size of the cell increases as well.

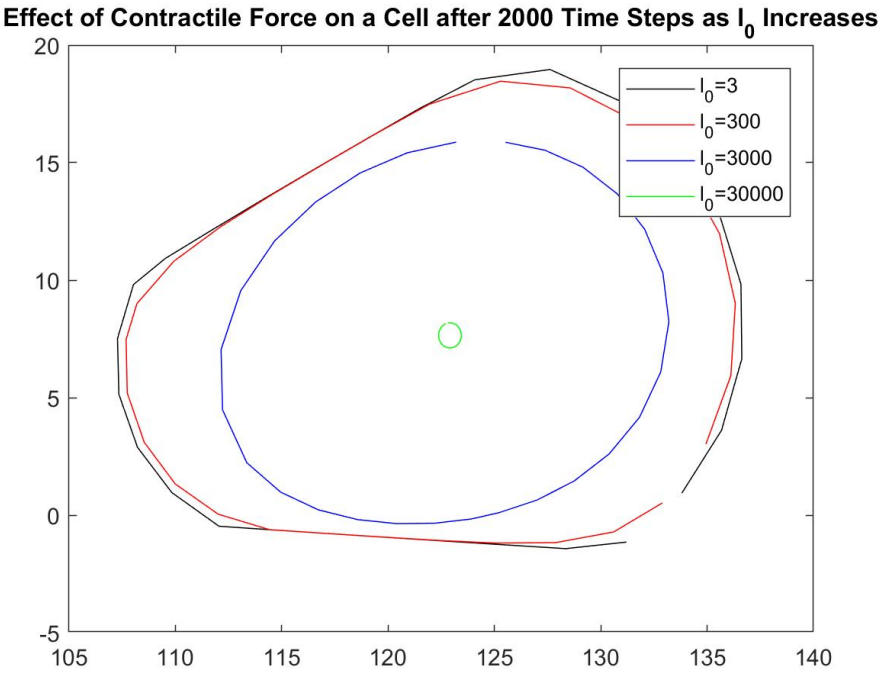

Figure 2.2 Graph showing how the value of ℓ_0 affects the contractile force. Each cell started with the same initial condition, and the contractile force was used to update the positions of the vertices for 2000 time steps. Note that as the value of ℓ_0 increases, the size of the cell decreases.

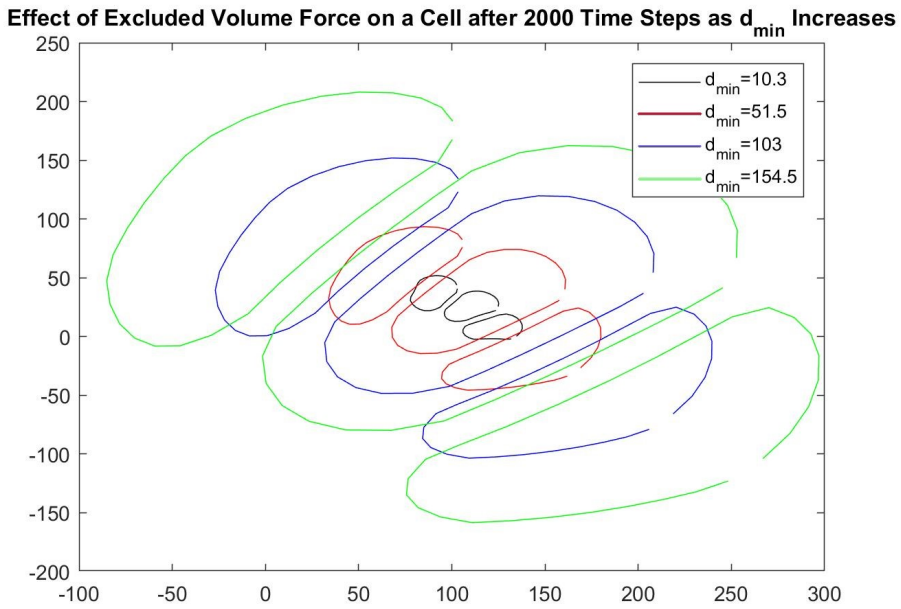

Figure 2.3 Graph showing how the value of d_{min} affects the excluded volume force. Each simulation of three cells had the same initial condition, and the excluded volume force was used to update the positions of the vertices for 2000 time steps. Note that as the value of d_{min} increases, the vertices spread out farther, resulting in larger cells and larger distances between cells.

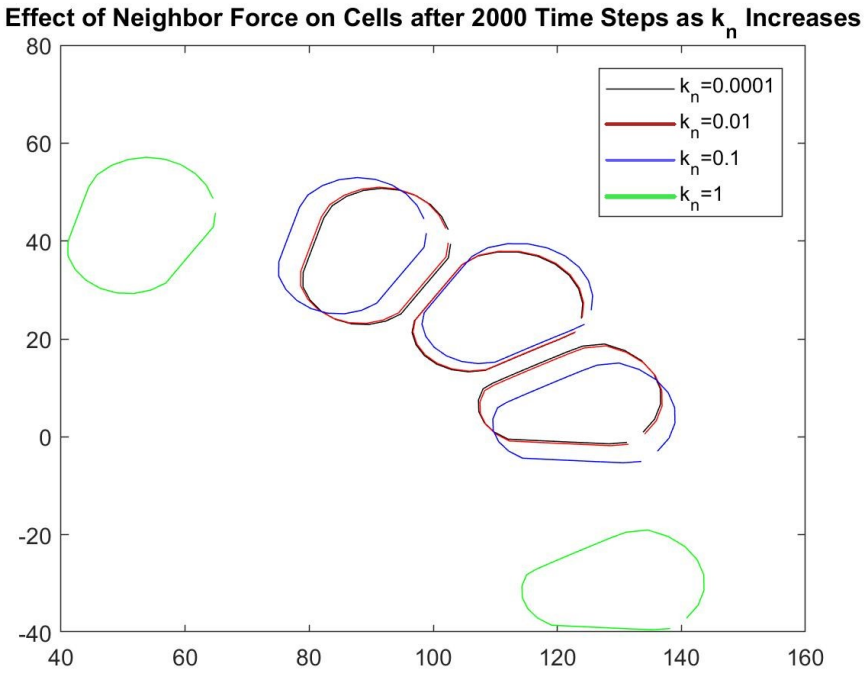

Figure 2.4 Graph showing how the value of k_n affects the neighbor force. Each simulation of three cells had the same initial condition, and the neighbor force was used to update the positions of the vertices for 2000 time steps. Note that as the value of k_n increases, the neighbor force strengthens.

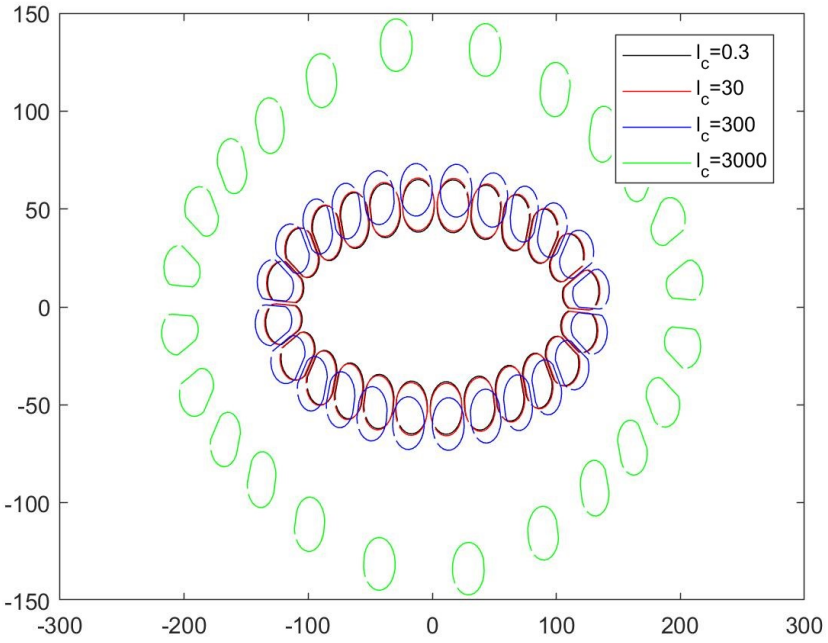

Figure 2.5 Graph showing how the value of ℓ_c affects the central force. Each simulation had the same initial conditions, and the central force was used to update the positions of the vertices for 2000 time steps. Note that as the value of ℓ_c increases, the cells spread out from the center, resulting in larger distances between cells.

Chapter 3

Cellular Proliferation

3.1 Cell-Division Cycle

As mentioned in Chapter 1, every cell in the model will be in one of three states related to the cell-division cycle: interphase, mitosis, or G_0. When a cell is in interphase, a timer is counting down after each time step. Once the interphase timer has finished, the cell will start a mitosis timer. The interphase timer is four times as long as the mitosis counter. Once the mitosis timer has finished, the cell will undergo a check for whether the cell will divide. This check will be discussed in the next two sections, but once the check occurs, the cell will either fail the check and not divide, or will pass the check and undergo division. If a cell does not divide, then the cell will start over in the cell-division cycle and will start the interphase timer. A cell that does divide will produce two daughter cells along the shortest chord that crosses through the cell's centroid. Both of the resulting cells will either start an interphase timer, or enter the G_0 state.

In addition to the interphase and mitosis timers, every cell has a generation counter. If a cell divides, then both of the resulting cells will be of the next generation after the generation of the original cell. For example, every cell starts as generation 0. If a generation 0 cell divides, then the two resulting cells will be generation 1 cells. Any cell that reached generation 5 will enter the G_0 state and will no longer be able to divide. A cell in the G_0 state will not have an interphase or mitosis counter and will stay in the G_0 state.

3.2 Signalling Gradients and Division Probability

Chapter 1 discussed the establishment of a signalling gradient in the model to simulate the effects of FGF and SHH on cellular proliferation. Recall that each source of FGF or SHH had an area of effect in which the probability of a cell dividing was influenced. Once a cell's mitosis timer has finished, the cell will undergo a check to determine whether the cell will divide. The probability of whether a cell will pass this check is determined by the location of the cell's centroid. Every cell will fall under one of the following catagories: the cell's centroid will only be in the area of effect for the FGF source, the cell's centroid will only be in the area of effect for the permanent SHH source, the cell's centroid will only be in the area of effect for the disappearing SHH source, the cell's centroid is in the area of effect for multiple signalling proteins, or the cell's centroid is outside the area of effect of all three sources.

3.2.1 Cells Only Influenced by FGF Source

Recall that the FGF source is a line segment with vertices at the points $\mathbf{v}_1$ and $\mathbf{v}_2$. Let p_f be the maximum probability of a cell passing the division check inside the area of effect for the FGF source, and let p_{min} be the probability of a cell dividing outside of the areas of effect for the FGF source and SHH sources such that $0 \leq p_{min} < p_f \leq 1$. Let r_f be the radius of the area of effect for the FGF source. The probability of a cell passing a division check decreases linearly as the centroid of the cell moves away from the center of the area of effect for a signalling protein until the centroid of the cell is a distance of r_f away from the FGF source. Then the probability of a cell dividing within the area of effect of the FGF source is

$$p_1(\mathbf{c}) = p_f \left(1 - \frac{1}{r_f} \min_{\tau \in [0,1]} ||\mathbf{c} - \tau\mathbf{v}_1 - \mathbf{v}_2(1-\tau)||\right) + \frac{p_{min}}{r_f} \min_{\tau \in [0,1]} ||\mathbf{c} - \tau\mathbf{v}_1 - \mathbf{v}_2(1-\tau)||, \tag{3.1}$$

where $\mathbf{c}$ is the location of the cell's centroid and $||\cdot||$ denotes the Euclidean norm.

3.2.2 Cells Only Influenced by Permanent SHH Source

Recall that there are two SHH point sources in the model. One source is permanent for the purposes of the model while the other source is disappearing. Let $\mathbf{s}_1$ be the location of the permanent point source. Let $p_{s,1}$ be the maximum probability of a cell passing the division check inside the area of effect for the permanent SHH point source, and let $r_{s,1}$ be the radius of the area of effect for the permanent SHH source. Like the FGF source, the probability of a cell influenced by this source decreases linearly as the distance between the cell's centroid and the SHH point source until the probability reaches p_{min} when the distance between the point source and the cell's centroid is $r_{s,1}$. Then the probability of a cell dividing within the area of effect of the permanent SHH source is

$$p_2(\mathbf{c}) = p_{s,1}\left(1 - \frac{1}{r_{s,1}}\left|\left|\mathbf{c} - \mathbf{s}_1\right|\right|\right) + \frac{p_{min}}{r_{s,1}}\left|\left|\mathbf{c} - \mathbf{s}_1\right|\right|. \tag{3.2}$$

3.2.3 Cells Only Influenced by Disappearing SHH Source

The disappearing SHH source will not disappear immediately because older SHH from that point source continues to diffuse after the point source ceases to produce SHH. Instead, a second, smaller circle will grow inside the area of effect as time progresses in the simulation. The smaller circle will represent the region where the last of the old SHH has diffused and was not replaced with new SHH. Let s_2 be the location of the disappearing point source. Let $r_{s,2}$ be the radius of the area of effect for the SHH, and let $r_{s,3}$ be the radius of the smaller circle. Then a cell will only be influenced by this SHH source if

$$r_{s,3} < \left|\left|\mathbf{c} - \mathbf{s}_2\right|\right| < r_{s,2}$$

The SHH source will completely disappear when $r_{s,2} = r_{s,3}$. Let $p_{s,2}$ be the maximum probability of a cell passing the division check inside the area of effect for the disappearing SHH source. Then the probability of a cell dividing within the area of effect

of the disappearing SHH source is

$$p_3(\mathbf{c}) = p_{s,2}\left(1 - \frac{1}{r_{s,2}}\left|\left|\mathbf{c} - \mathbf{s}_2\right|\right|\right) + \frac{p_{min}}{r_{s,2}}\left|\left|\mathbf{c} - \mathbf{s}_2\right|\right|. \tag{3.3}$$

3.2.4 Cells Influenced by Multiple Signalling Gradients or No Signalling Gradients

If a cell has a centroid that is in the area of effect for multiple sources, then all relevant probabilities will be calculated, and the cell will undergo one division check for each source that is influencing it. If the cell passes at least one check, then the cell will divide. For example, if a cell has a centroid at $\mathbf{c}$ such that the cell is in the areas of effect for the FGF and permanent SHH sources, then the cell will undergo one check using the probability calculated using Eq. (3.1) and then a second check using the probability calculated using Eq. (3.2). If it passes one or both of the checks, then the cell will divide. If a cell is not in the area of effect for any of the sources, however, then the cell will only undergo one division check and will have a probability of passing the division check of p_{min}.

3.3 Implementation of Division Check

Let x be a uniformly distributed random variable from the distribution $X \sim U(0, 1)$. A new value of x will be sampled for each check that is performed. Let p be the probability of the cell passing the check. Then the cell will pass the division check if $x \leq p$ and will fail the division check if $x > p$. If a cell is influenced by multiple signalling proteins, then the number of division checks that the cell will undergo will be the same as the number of signalling proteins influencing the cell, with a new value of x being sampled for each check. Table 3.1 shows every possible results for a division check for a cell under the influence of zero, one, two, and all three signalling proteins. Note that a cell influenced by zero or one signalling proteins undergoes one check, a cell influenced by two signalling proteins undergoes two checks, and a cell

influenced by three signalling proteins undergoes three checks. In Table 3.1, each row gives the results of each check, and the rightmost column states whether the cell will divide or not. Note that a cell will divide if it passes at least one check, and a cell will not divide only if it fails every check.

Table 3.1 Division Check for Cells of Influenced by Signalling Proteins

Number of Signalling Proteins	Check 1?	Check 2?	Check 3?	Cell Divide?
0	Yes			Yes
	No			No
1	Yes			Yes
	No			No
2	Yes	Yes		Yes
	Yes	No		Yes
	No	Yes		Yes
	No	No		No
3	Yes	Yes	Yes	Yes
	Yes	Yes	No	Yes
	Yes	No	Yes	Yes
	Yes	No	No	Yes
	No	Yes	Yes	Yes
	No	Yes	No	Yes
	No	No	Yes	Yes
	No	No	No	No

Chapter 4

Model Analysis

4.1 Progression of Model Development

The model on which this work was built upon consisted of the three vertex-unique forces and a less-detailed version of cellular proliferation. While the vertex-unique forces are important to the current model, these forces were not able to account for factors addressed by the cell-unique forces. The area force and contractile force were able to regulate cell size and the excluded volume force was able to combat problems such as overlapping vertices, these forces were not able to keep stem cells grouped together nor preserve Rathke's pouch. The addition of the neighbor force was able to preserve connections between nearby cells, and the central force was able to prevent drifting and maintain Rathke's pouch.

The development of more detailed cellular division procedures greatly improved the model's accuracy in simulating cellular proliferation. The early version of the model guaranteed a cell would divide once its mitosis timer finished, and no signalling gradients were accounted for in the model. The current model now has a system of signalling gradients in place to more accurately simulate cellular proliferation as well as to offer a system to build upon to allow this model to study cellular differentiation.

4.2 Analysis of Current Model

Currently, this model is designed to run simplified simulations of cellular proliferation in a developing pituitary gland. However, it is not yet clear what values should be

used for the constants in the equations from Chapter 2 to balance the forces. Once the correct values for these constants are found, the model proposed in this thesis will be able to more accurately simulate cellular proliferation in the simplified Rathke's pouch. The cellular proliferation infrastructure should allow for the addition of cellular diversification and specialization, an aspect of research this model is currently not designed to study.

Figure 4.1 shows results of a simulation that started with the configuration of cells and signalling gradients depicted in Figure 1.4. The effects of the signalling gradients is apparent, as the cells in the anterior and posterior regions of Rathke's pouch have divided more often than other regions. This was to be expected, as these cells would be closest to the centers of the proteins' areas of effect. However, the daughter cells are not moving from where they divided, retaining the shape they had when they finished dividing. This means that either the area force is not strong enough to move the cells or the cells are dividing too quickly.

Although some of the features added to this model, such as the central force and neighbor force, allowed for one to account for more aspects of pituitary organogenesis, these new features still oversimplify the phenomena they were designed to simulate. For example, the neighbor force assumes that all cells in the pituitary gland have the same attraction to one another. However, epithelial cells are connected to each other with greater force than mesenchymal cells, which have the potential to migrate through the gland. Without changing the implementation of this force, the neighbor force will not be able to accurately simulate epithelial cells and mesenchymal cells under the same simulation parameters. However, if the neighbor force was altered to have different k_n values for different types of cells, this issue would likely be less prominent.

4.3 Other Mathematical Models of Organogenesis

Although mathematical models of pituitary organogenesis are not well-documented at this time, organogenesis models have been studied for other organs such as the lungs and kidneys. However, these mathematical models must deal with a different challenge than this model attempted to solve at this point in it's development. During development, mouse lungs develop thousands of branches that form in a stereotyped process (Wittwer et al. 2016). Kidney models attempt to simulate a branching process as well (Zubkov et al. 2015). In simulating the three-dimensional development of lungs, Wittwer et al. used a phase field method to simulate the partial differential equations involved in modeling lung organogenesis and concluded that the method would be useful for their future lung development models (Wittwer et al. 2016). To simulate kidney organogenesis, Zubkov et al. used a spacially-averaged, time dependent model and were able to use this model to make predictions about the final branch generation number under normal and some perturbed conditions (Zubkov et al. 2015). A mathematical model of organogenesis that did not focus on branching was Setty et al. in a model of pancreatic organogenesis in mice (Setty et al. 2008). The model produced by Setty used statecharts to dictate how cells would behave under certain circumstances through a hierarchy of states (Setty et al. 2008).

Although these models were concerned about branching in the lungs and kidneys, something this model was not designed to consider yet, these methods may have potential in helping to simulate the growth of blood vessels in the anterior lobe of the pituitary gland once this model is developed enough to begin simulating such development. The statecharts used by Setty et al. could potentially be used in this model to account for differentiation. Although the differentiation stem cells undergo in the pancreas is different than what stem cells undergo for the anterior lobe of the pituitary gland, one might be able to implement a similar hierarchy of states to dictate how specific stem cells differentiate.

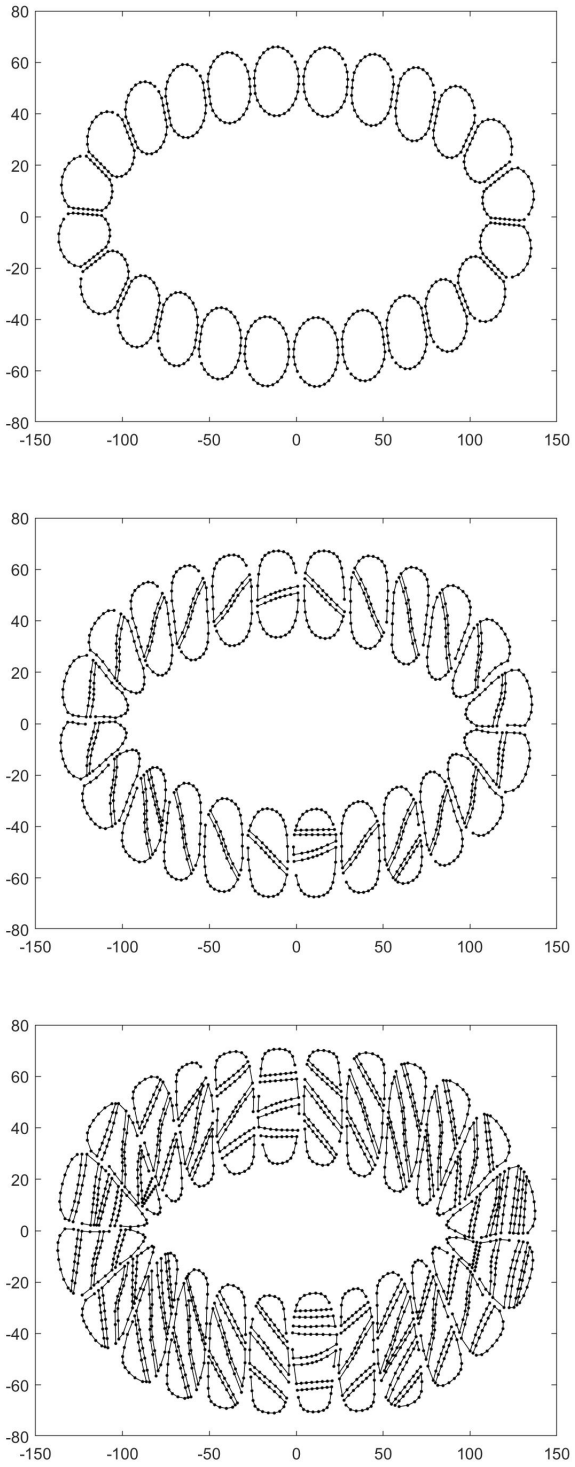

Figure 4.1 (Top) Initial configuration for simulation. (Middle) Configuration after 400 time steps. (Bottom) Configuration after 800 time steps.

Chapter 5

Conclusion

The goal of the model proposed in this thesis was to simulate the proliferation of stem cells in a simplified Rathke's pouch and to test whether signalling gradients of FGF and SHH affect the shape of the anterior lope of the pituitary gland as it develops. The proposed model has the infrastructure needed to simulate the proliferation of the stem cells in a simplified Rathke's pouch, although further study will be needed to determine what values to use for k_a, a_0, k_ℓ, ℓ_0, d_{min}, k_n, k_c, and ℓ_c from Eq. (2.4), Eq. (2.5), Eq. (2.6), Eq. (2.8), and Eq. (2.9). Thus, at this time, the model is not able to accurately test how the signalling gradients affect the shape of the anterior lobe of the pituitary gland as it develops until the values for these constants are found. This model also provides an infrastructure that can be used to study more detailed systems of pituitary organogenesis. Thus, future work for this project would be to determine the appropriate simulation parameter values and to implement new features to allow for cellular diversification and the use of signalling gradients to influence cellular diversification.

Bibliography

Björklund, Mikael and Samuel Marguerat (2017). "Editorial: Determinants of Cell Size". In: *Frontiers in Cell and Developmental Biology* 5, p. 115. ISSN: 2296-634X. DOI: 10.3389/fcell.2017.00115. URL: https://www.frontiersin.org/article/10.3389/fcell.2017.00115.

Boromand, Arman et al. (Dec. 2018). "Jamming of Deformable Polygons". In: *Phys. Rev. Lett.* 121 (24), p. 248003. DOI: 10.1103/PhysRevLett.121.248003. URL: https://link.aps.org/doi/10.1103/PhysRevLett.121.248003.

Fletcher, Alexander G. et al. (2013). "Implementing vertex dynamics models of cell populations in biology within a consistent computational framework". In: *Progress in Biophysics and Molecular Biology* 113.2, pp. 299–326. ISSN: 0079-6107. DOI: https://doi.org/10.1016/j.pbiomolbio.2013.09.003. URL: https://www.sciencedirect.com/science/article/pii/S0079610713000989.

Scully, Kathleen M. and Michael G. Rosenfeld (2002). "Pituitary Development: Regulatory Codes in Mammalian Organogenesis". In: *Science* 295.5563, pp. 2231–2235. ISSN: 0036-8075. DOI: 10.1126/science.1062736. eprint: https://science.sciencemag.org/content/295/5563/2231.full.pdf. URL: https://science.sciencemag.org/content/295/5563/2231.

Setty, Yaki et al. (2008). "Four-dimensional realistic modeling of pancreatic organogenesis". In: *Proceedings of the National Academy of Sciences* 105.51, pp. 20374–20379. ISSN: 0027-8424. DOI: 10.1073/pnas.0808725105. eprint: https://www.pnas.org/content/105/51/20374.full.pdf. URL: https://www.pnas.org/content/105/51/20374.

Shields, Rachel et al. (2015). "Magnetic resonance imaging of sellar and juxtasellar abnormalities in the paediatric population: an imaging review". In: *Insights into Imaging* 6.2, pp. 241–260. DOI: 10.1007/s13244-015-0401-5.

Wilfinger, William W. et al. (1984). "An in vitro model for studies of intercellular communication in cultured rat anterior pituitary cells". In: *Tissue and Cell* 16.4, pp. 483–497. ISSN: 0040-8166. DOI: https://doi.org/10.1016/0040-8166(84)90026-0. URL: https://www.sciencedirect.com/science/article/pii/0040816684900260.

Wittwer, Lucas Daniel et al. (2016). *Simulating Organogenesis in COMSOL: Phase-Field Based Simulations of Embryonic Lung Branching Morphogenesis*. arXiv: 1610.09189 [q-bio.QM].

Youngblood, Julie L, Tanner F Coleman, and Shannon W Davis (2018). "Regulation of Pituitary Progenitor Differentiation by β-Catenin". In: *Endocrinology* 159.9, pp. 3287–3305. DOI: 10.1210/en.2018-00563.

Zubkov, V.S. et al. (2015). "A spatially-averaged mathematical model of kidney branching morphogenesis". In: *Journal of Theoretical Biology* 379, pp. 24–37. ISSN: 0022-5193. DOI: https://doi.org/10.1016/j.jtbi.2015.04.015. URL: https://www.sciencedirect.com/science/article/pii/S0022519315001782.